A Diameter-Selective Chiral Separation of Single-Wall Carbon Nanotubes Using Nitronium Ions

KAY HYEOK AN,[1] CHOL-MIN YANG,[1] JI YEONG LEE,[1] SEONG CHU LIM,[1] CHUL KANG,[2] JOO-HIUK SON,[2] MUN SEOK JEONG,[3] and YOUNG HEE LEE[1,4]

1.—BK21 Physics Division, Institute of Basic Science, Center for Nanotubes and Nanostructured Composites, Sungkyunkwan Advanced Institute of Technology, Sungkyunkwan University, Suwon 440-746, Korea. 2.—Department of Physics, University of Seoul, Seoul 130-743, Korea. 3.—Advanced Photonics Research Institute, Gwangju Institute of Science and Technology, Gwangju 500-712, Korea. 4.—E-mail: leeyoung@skku.edu

We propose a method for a diameter-selective removal of metallic single-walled carbon nanotubes (m-SWCNTs) from semiconducting (s-) ones. Our separation technique is capable of 100% separation of semiconducting and metallic nanotubes for small diameter nanotubes. We dispersed SWCNT powder by sonication in a mixed solution of tetramethylene sulfone and chloroform, where nitronium ions were well dissolved. Positively charged nitronium ions were intercalated into nanotube bundles, where the intercalation was promoted also by the counter ions. Nitronium ions selectively attacked the sidewall of m-SWCNTs due to the abundant presence of electron density at the Fermi level, thus yielding stronger binding energy compared to the counterpart s-SWCNTs. The s-SWCNTs were left on the filter after filtration, whereas m-SWCNTs were perfectly destroyed by nitronium ions and drained away as amorphous carbons. This preferable adsorption became obscured for nanotubes with diameters greater than 1.1 nm. The effectiveness of removing m-SWCNTs was confirmed by the transmission electron microscope observations, x-ray photoemission spectra, resonant Raman spectra, and absorption spectra.

Key words: Carbon nanotube, nitronium hexafluoroantimonate, nitronium tetrafluoroborate, chiral separation, resonant Raman spectra

INTRODUCTION

The electronic structure of carbon nanotubes is determined by their chirality and diameter, which are not selectively controlled by conventional synthesis approaches. The present state of art technology for carbon nanotube synthesis always produced samples with mixing chiralities. The coexistence of metallic (m-SWCNTs) and semiconducting single-walled carbon nanotubes (s-SWCNTs) in commercially available samples has been a bottleneck for much fundamental research and applications with high device performance, such as nanotransistors, memory devices, and chemical/bio-nanosensors. Post-treatments of samples are necessary to selective chirality separation for high performance and reproducibility of devices. Several methods of separating semiconducting nanotubes from metallic ones or vice versa using dielectrophoresis, octadecylamine (ODA), bromination, and deoxyribonucleic acid (DNA) have been reported.[1–5] The dielecrophoresis method requires a priori nanodispersion of nanotubes for high yield of separation and may not be scalable to large quantity treatment. Preferential adsorption of ODAs on semiconducting nanotubes can give rise to high separation yield with large quantity, but extra work is necessary to remove additives. The bromination approach is easy and straightforward to understand but leaves a poor separation yield. Therefore, a realistic separation method for high yield and massive quantities of specific metallicity is still lacking.

Another approach is the functionalization that leads to transformation of the electronic structures of nanotubes. Strong chemisorption by hydrogenation and fluorination transformed electronic structures from m-SWCNTs to s-SWCNTs by inducing a

(Received February 19, 2005; accepted June 17, 2005)

partial sp^3 hybridization.[6,7] This sometimes deteriorated the nanotube walls, leading to a disintegration into amorphous carbons or graphitic layered structures.[8] The diazonium salts have also been introduced to react with the nanotubes to extract electrons from nanotubes in the formation of a covalent aryl bond, demonstrating chemoselective reactions with metallic versus semiconducting nanotubes.[9] Thermal annealing of the diazonium-treated nanotubes at 300°C cleaved the aryl moieties from the sidewalls and recovered the spectrocopic signatures of the pristine nanotubes. Small-diameter nanotubes have been selectively removed by an oxidative etching particularly with the assistance of light illumination.[10,11]

Our aim is to select semiconducting nanotubes from metallic ones in a large quantity with high yield and more importantly without affecting nanotube properties so that the selected nanotubes could be used directly for various applications. Here, we report a new method of destroying small-diameter m-SWCNTs from s-SWCNTs by dispersing SWCNT powder in tetramethylene sulfone (TMS)/chloroform solution with nitronium ions (NO_2^+). This method is simple and straightforward without altering electronic structures after treatment, and furthermore it is easily scalable for the large quantity of SWCNTs with high separation yield.

EXPERIMENTAL PROCEDURE

Nitronium hexafluoroantimonate (NO_2SbF_6: NHFA) or nitronium tetrafluoroborate (NO_2BF_4: NTFB) of 40 mmol was dissolved in TMS/chloroform (1:1 by weight) solution of 100 mL. The nitronium salts were ionized in the mixed solvent as follows:

$$NO_2SbF_6 \rightarrow NO_2^+ + SbF_6^- \text{ or } NO_2BF_4 \rightarrow NO_2^+ + BF_4^-$$

where both reactions produced nitronium ions.

The pristine HiPCO SWCNT soot of 10 mg purchased from Carbon Nanotechnologies Inc. (Houston, TX) was suspended by sonicating for 24 h in the prepared NHFA or NTFB solution at 60°C. After reaction, the suspension was filtered using a membrane filter with a pore diameter of 10 μm and then washed with an ethanol several times. The residual SWCNTs on the filter treated with NHFA or NTFB solution were dried in vacuum at 100°C overnight, and were further heat treated in a vacuum at 1,000°C for 30 min. Figure 1 shows the sequence of procedures for the sample treatment.

The metallicity of samples was characterized by the resonant Raman spectroscopy (Renishaw, microprobe RM1,000) with several wavelengths of 514.5 nm (Ar^+ ion laser), 632.8 nm (He-Ne laser), and 785 nm (diode laser). Samples were further analyzed by the field-emission scanning electron microscope (FESEM; JEOL 6700F, Japan Electron Optics Ltd., Tokyo) and field emission JEOL 2010F high-resolution transmission electron microscope (HR-TEM, 200 keV). X-ray photoemission spectroscopy (XPS) was carried out using a PHI 5,100 spectrometer (Perkin Elmer Instruments, Oak Ridge, TN) using a Mg K_α (1253.6 eV) line. The SWCNT powder was immersed in isopropanol solution and sonicated for dispersion for 4 h for absorption measurements. This solution was then dropped on a quartz plate and the absorption spectra were obtained by using a UV-vis-NIR spectrophotometer (Hitachi U-3501, Japan).

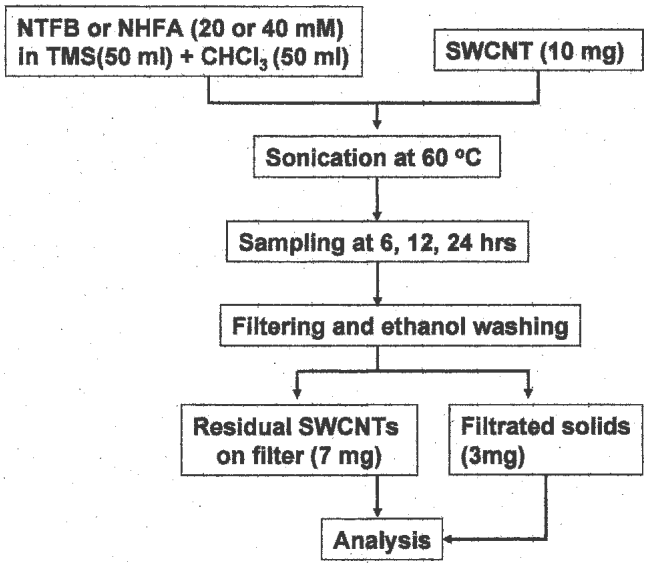

Fig. 1. Schematic experimental procedure of the NHFA and NTFB treatments of the SWCNTs.

RESULTS AND DISCUSSION

Figure 2 shows the FESEM and HRTEM images of the pristine SWCNTs, residual SWCNTs on filter, and filtrated solids. Bundles of the pristine SWCNTs were randomly entangled with a broad diameter distribution of 5–30 nm, as shown in Fig. 2a and b. However, the bundle sizes of the residual SWCNTs on the filter were enlarged due to an aggregation effect in solution, as presented in Fig. 2c and e, without distinct deformation of the nanotube walls, confirmed by the HRTEM images (Fig. 2d and f). On the other hand, the morphology of the filtrated (precipitated) solids appeared somehow completely different from that of the pristine SWCNTs (Fig. 2g). The SWCNT bundles were hardly seen and mostly fragmented into small pieces, forming carbonaceous particles, as observed in Fig. 2h. Small graphitic flakes in addition to the majority of amorphous carbons were also visible, again evidence of disintegration of nanotube walls. We emphasize that simply dispersed pristine SWCNTs in TMS/chloroform without NHFA or NTFB treatment were not filtrated through the membrane filter with a pore diameter of 10 μm. Only nanotubes disintegrated by the NHFA were filtrated through the filter. Similar trends were observed with the NTFB treatment. It has been well known that the graphite surface can be attacked easily by nitronium ions at the graphite surface.[12] The nitronium ions are capable of capturing the available π electrons in the (metallic) graphite, enhancing the binding energy with graphite surface. Because the SWCNTs also have similar π

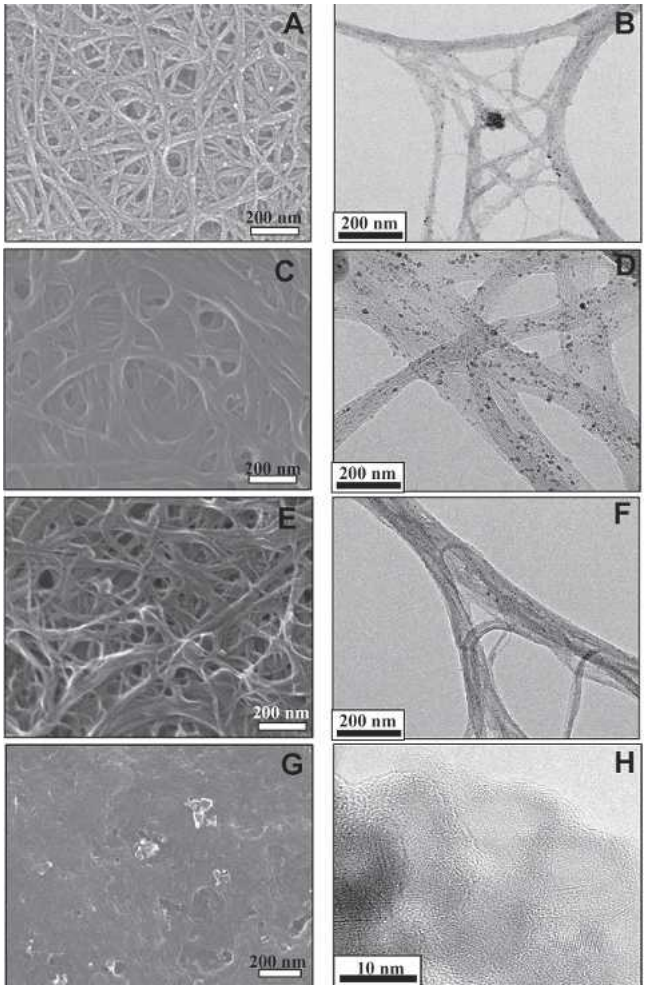

Fig. 2. FESEM and HRTEM images of (a) and (b) pristine SWCNTs, (c) and (d) residual SWCNTs treated with NHFA, and NTFB on (e) and (f) filter and (g) and (h) filtrated solids after sonication for 24 h in TMS/chloroform with 40 mmol of NHFA, respectively.

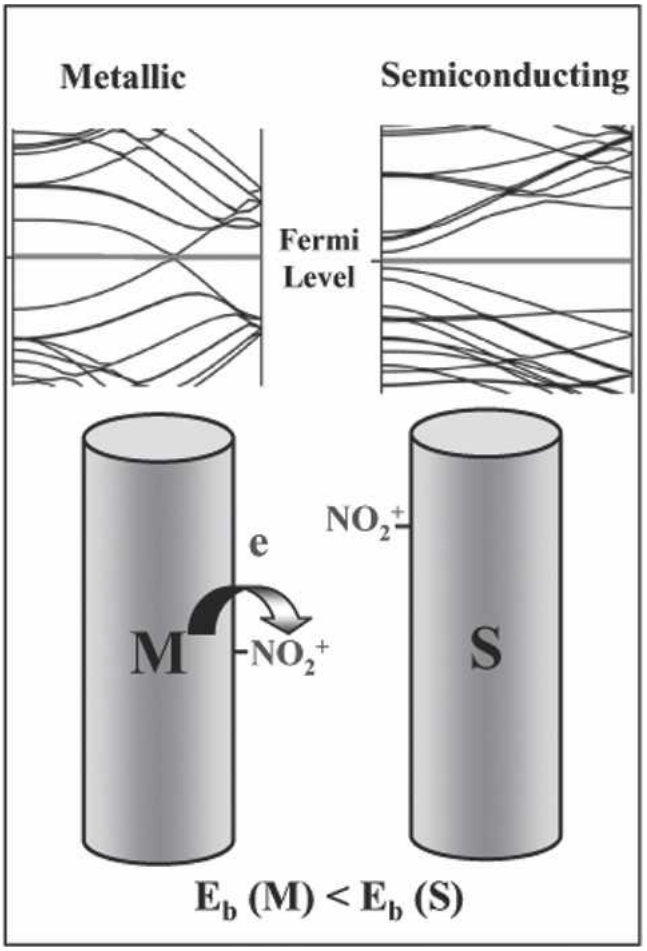

Fig. 3. The schematic band structures of metallic and semiconducting nanotubes (top) and the schematic diagram of the preferential binding of nitronium ion on metallic tube (bottom).

electrons on the surface except the strain effect, we expect that the nitronium ions can attack π electrons on the nanotube wall and thus provoke stable adsorption. The availability of the electrons at the Fermi level is a key factor in determining the binding nature, similar to the diazonium effect.[9] Because m-SWCNTs have more abundant electron charge density at the Fermi level than the counterpart s-SWCNTs, it is easy for m-SWCNTs to lose their electrons to the positively charged nitronium ions (Fig. 3). This will enhance the binding energy compared to the counterpart m-SWCNTs. We therefore expect that nitronium ions can be adsorbed more strongly on m-SWCNT sidewalls than on s-SWCNT ones. Once nitronium ions are adsorbed on nanotube walls, similar to graphite intercalation from either the nitrogen or oxygen side, they will be squeezed between bundles to enhance the binding energy. Strong adsorption of nitronium ions particularly from oxygen species may attack m-SWCNT sidewalls and furthermore disintegrate the nanotube walls, similar to an oxidative etching process that may lead to graphitic flakes[13] or amorphous carbons, as observed in our experiments.

The selective disintegration of m-SWCNTs involves strong chemisorption with nitronium ions. The evidence of chemisorption of nitronium ions to the sidewall of m-SWCNTs was observed in XPS data. The C1s XPS spectrum of the pristine SWCNTs showed two components, as shown in Fig. 4a. The peak around 284.5 eV represented sp^2-hybridized carbons on the tube wall, which is comparable to the C1s binding energy of graphite. The small peak around 285.3 eV was related to sp^3-hybridized carbons that may originate from the presence of defects on the tube walls or nanotube ends.[14] After NHFA treatment, these peaks of the residual SWCNTs on the filter were broadened and downshifted by about 1 eV (middle panel), indicating a strong charge transfer on adsorbates that was provoked between nanotubes and nitronium ions during adsorption. In addition, three small peaks were newly developed at 285.4, 287.4, and 288.3 eV, which were assigned to C-N, C-O, and C-F bonds, respectively.[7,14,15] These peaks disappeared after heat treatment. This shift was completely recovered with similar full-widths at half-maximum to that of

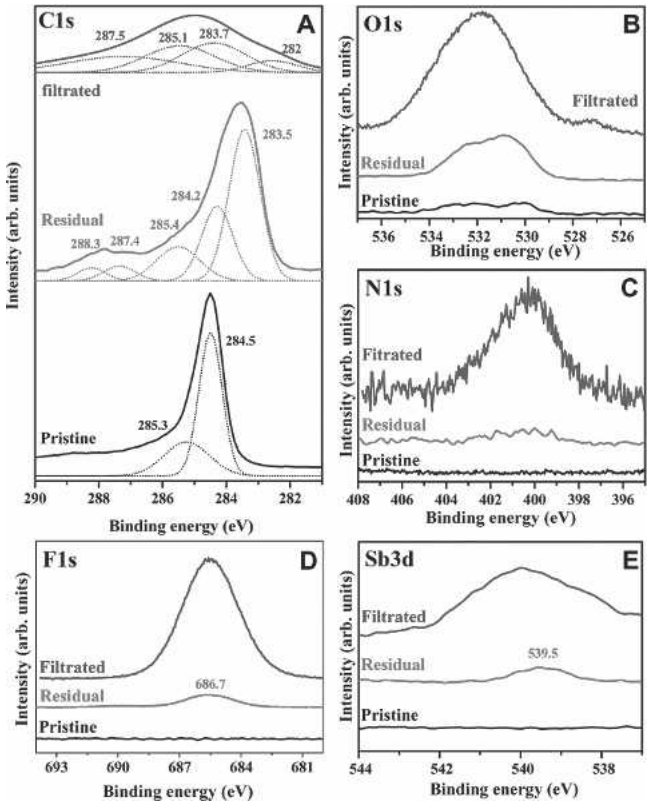

Fig. 4. XPS spectra of C1s with (a) Gaussian curve fittings, (b) O1s, (c) N1s, (d) F1s, and (e) Sb3d for the pristine sample, residual SWCNTs on filter, and filtrated solids after sonication for 24 h in TMS/chloroform with 40 mmol of NHFA, respectively.

the pristine sample after heat treatment at 1,000°C in a vacuum. On the other hand, full-widths at half-maximum of the precipitated solids became extraordinarily broadened (top panel) and furthermore the ratio of sp^3-like bonds to sp^2-like bonds was significantly increased. The broad peak near 287.5 eV and the small peak near 282 eV (carbidic carbon),[16] together with the broadened main peaks, indicated the filtrated solids to be functionalized by various adsorbates. The broad peak was still preserved even after heat treatment. These findings led to the conclusion that the filtrated SWCNTs were disintegrated into amorphous carbons, in good agreement with the SEM and TEM morphology for the filtrated solids (Fig. 2g and h). Interestingly, the amount of the sample loss after filtration was about 25–30 wt.%, close to the theoretically estimated metallic content.

In the O1s XPS spectrum of the pristine SWCNTs, the presence of ambient oxygen species was observed in Fig. 4b. The oxygen-related peaks of the residual SWCNTs were developed with NHFA treatment due to the abundant adsorption of nitronium ions. This peak was again mostly removed after heat treatment. The oxygen-related peak was highly developed in the precipitated sample, indicating the ambient presence of defect states. The similar behavior in the residual SWCNTs was also observed with N1s, F1s, and Sb3d spectra. The C-N related and N-O related peaks were observed near 402.5–396.5 eV from N1s spectra (Fig. 4c).[16] Ionic C-F bonds near 686.7 eV were developed in the residual SWCNTs (Fig. 4d).[17] We also observed a SbO_x-related peak in Fig. 4e near 539.5 eV in the NHFA-treated SWCNTs due to intercalation of hexafluoroantimonate ions into the SWCNT bundles.[18] Yet SbO_x-related materials were also removed during heat treatment at 1,000°C in vacuum. Surprisingly, the oxygen, nitrogen, fluorine, and antimony-related peaks of the filtrated solids dramatically increased compared to that of the residual SWCNTs. We emphasize that the filtrated solids were more severely attacked than the residual SWCNTs. It is clear that strong adsorption of nitronium ions disintegrate the m-SWCNT walls, due to more abundant electron charge density at the Fermi level than the counterpart s-SWCNTs.

In order to compare the reactivity between NTFB and NHFA, we investigated the resonant Raman spectra of the residual SWCNTs treated at 20 mmol of NTFB and NHFA as a function of treated times, as shown in Fig. 5. The numbers in Fig. 5 indicate the corresponding diameters from each peak determined by [$\omega\ (cm^{-1}) = 235/d\ (nm) + 9$].[19] The metallic and semiconducting bands indicated by the dotted square boxes were determined from the Kataura plot.[20] We identified five distinct peaks in the RBM mode from the pristine sample at an excitation energy of 514 nm in Fig. 5. The RBM bands can be grouped into two characters: semiconducting S_{33} band (183 cm^{-1} and 204 cm^{-1}) and metallic M_{11} band (244 cm^{-1}, 259 cm^{-1}, and 266 cm^{-1}).

In the case of NTFB, although the intensities of the metallic bands in RBM modes monotonously decreased with increasing treatment times, metallic bands did not completely disappear, as observed in Fig. 5a. On the other hand, the metallic bands of NHFA-treated SWCNTs significantly diminished even at short treatment times and completely disappeared at 24 h, as presented in Fig. 5b. The selective removal of metallic nanotubes can be also revealed from the G-band. The long tail at a lower energy side of G-band is a characteristic of the metallic component and should be fitted by the Breit–Wigner–Fano (BWF) line shape.[21] The BWF line shape was clearly observed in the pristine sample (Fig. 5b and d). The BWF line shape completely vanished in the NHFA-treated SWCNTs (Fig. 5d), whereas the metallic component in NTFB-treated SWCNTs remained until 24 h. We note that the reactivity of NTFB was less effective than that of NHFA. This implies that the counter anion also plays an important role during reaction as an intercalator into the bundle. The anion size (SbF_6^-) of the NHFA is larger than the BF_4^- of NTFB, providing more room for nitronium ions to be intercalated into the bundle.

In order to clarify the nature of metallicity of the residual SWCNTs treated at 40 mmol of NHFA for 24 h, we investigated the resonant Raman spectra, as shown in Fig. 6. In an excitation energy of 514

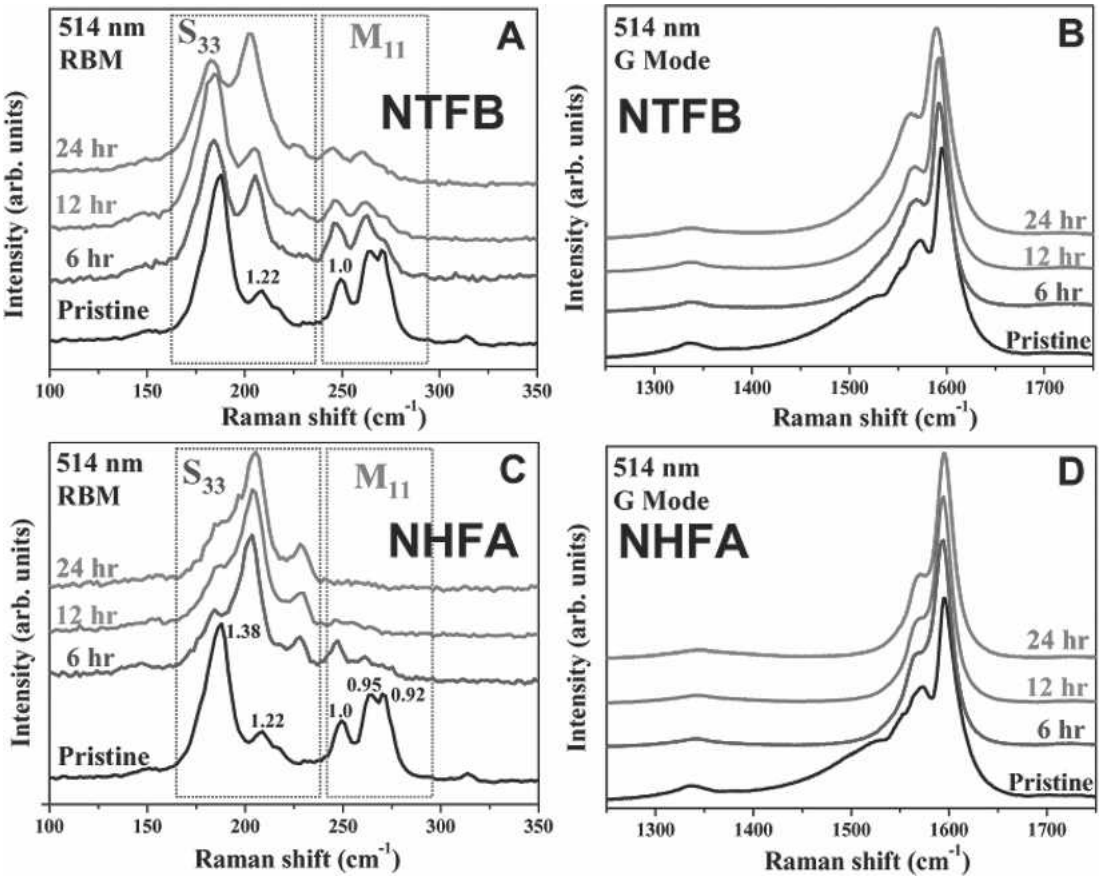

Fig. 5. RBMs and G-mode of Raman spectra as a function of treatment time with excitation energies of 514 nm for the pristine sample and the residual SWCNTs on the filter after 20 mmol of (a) and (b) NTFB and (c) and (d) NHFA treatment.

nm, the metallic band of the residual SWCNTs was completely removed after NHFA treatment, whereas the semiconducting peaks were slightly upshifted, as observed in Fig. 6a. This implies that nitronium ions could be adsorbed even on s-SWCNTs so as to upshift the peak positions due to the charge transfer to nitronium ions, in good agreement with the previously reported acceptor behavior.[7] After heat treatment at 1,000°C in vacuum, the peak shift of the semiconducting band was recovered and the peak was intensified, due to the removal of all of the adsorbates after heat treatment. However, the metallic band was still not visible. Therefore, the disappearance of the metallic band was not due to the shift of resonance by adsorbates, in good contrast with the previous works that the disappeared band in the RBM by the diazonium adsorption was recovered simply due to the desorption after heat treatment, leaving unaltered electronic structures of nanotubes.[9,22]

Figure 6b shows the RBM profiles at an excitation energy of 785 nm. In this case, we observed only the semiconducting S_{22} band (205 cm^{-1}, 216 cm^{-1}, 226 cm^{-1}, 234 cm^{-1}, and 267 cm^{-1}) from the pristine sample. The peak intensities of the large- (1.22 nm) and small- (0.92 nm) diameter nanotubes were reduced and the peak positions were slightly upshifted after NHFA treatment. The large-diameter nanotubes form a rather large interstitial space in the bundle to provide better accessibility for adsorbates.[23–25] On the other hand, in small-diameter nanotubes, the ratio of adsorbate to nanotube is high and furthermore large strain induces strong binding energy with adsorbates.[23–25] This provokes one to violate the resonance condition and shifts the peak positions. The related peak intensities were reduced as shown in the figure. These peaks were fully recovered again with similar intensity ratios and peak positions after heat treatment. The binding energy of nitronium ions to the sidewall of the semiconducting nanotubes was not strong enough to destroy nanotubes during adsorption and desorption, such that the electronic structures of s-SWCNTs remained unchanged after heat treatment. We emphasize here that s-SWCNTs with small diameters of 0.92 nm were not disintegrated after treatments, whereas the corresponding metallic band with diameters less than 1.1 nm was completely removed, as shown in Fig. 6a. This strongly suggests that the nitronium ions attacked selectively m-SWCNTs with small diameters less than 1.1 nm.

We also observed the Raman spectra with an excitation energy of 633 nm, as shown in Fig. 5c. In this case, the metallic bands at 216 cm^{-1} (1.16 nm) and 192 cm^{-1} (1.32 nm) and the semiconducting bands at 256 cm^{-1} (0.97 nm) and 281 cm^{-1} (0.88 nm) appeared in the pristine sample. The small-diameter (0.97 nm) s-SWCNTs were attacked to lead

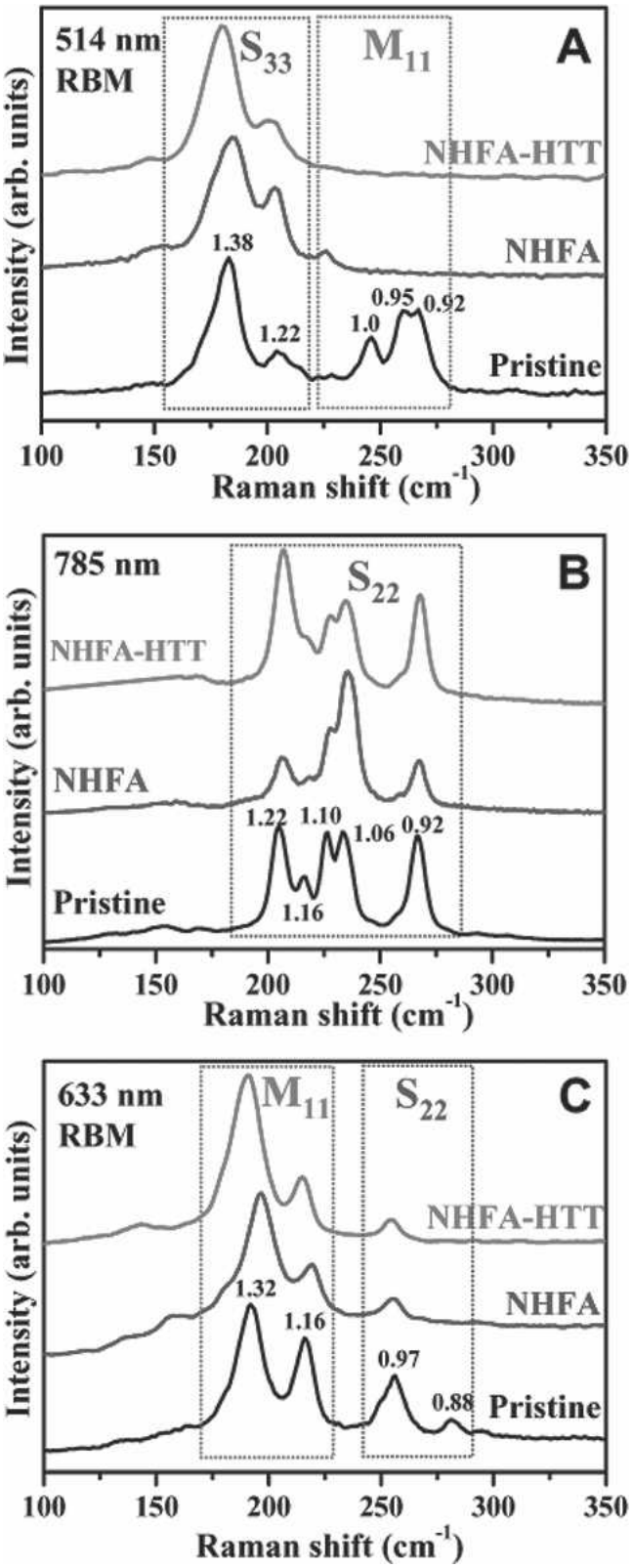

Fig. 6. RBMs of Raman spectra with excitation energies of (a) 514 nm, (b) 785 nm, and (c) 633 nm for the pristine sample, the residual sample on the filter after the 40 mmol of NHFA treatment by sonicating for 24 h (NHFA), and the residual sample with further heat treatment at 1,000°C (NHFA-HTT) in vacuum.

to a partial disintegration after NHFA and heat treatments, which is in good contrast with the completely recovered semiconducting peak of 0.92 nm at 785 nm. The semiconducting peak at 281 cm^{-1} (0.88 nm) completely disappeared. The strain is too large, 0.12 eV/atom in this case,[26] such that nanotubes can be disintegrated independent of the metallicity. The metallic bands were upshifted with NHFA treatment, confirming again an adsorption of nitronium ions. Although the metallic band at 216 cm^{-1} (1.16 nm) significantly decreased, the peak shift at 192 cm^{-1} (1.32 nm) was recovered again after heat treatment, similar to the semiconducting one in Fig. 6b. Yet, the preferable binding energy on m-SWCNTs to that of s-SWCNTs was not large enough to disintegrate m-SWCNTs, as predicted from theoretical calculations.[27] We have investigated NO_2 adsorption on single-walled carbon nanotubes using density functional calculations. We found that NO_2 adsorption on the sidewall of nanotubes was strongly electronic structure and strain dependent. NO_2 adsorption on metallic nanotubes was energetically more favorable than that on semiconducting nanotubes, and furthermore, the adsorption became less stable with increasing diameters of nanotubes. The adsorption barrier height of the metallic nanotube was lower than that of the semiconducting one, in which the barrier height became higher with increasing diameters, implying that the selective adsorption is not only energetically controlled but also kinetically controlled with strong diameter dependence. Our theoretical model explains well the recent experimental results on the selective removal of metallic nanotubes using nitronium ions and can be a good guideline for the separation of nanotubes by electronic structures using various adsorbates. The selective attack of metallic nanotubes became unclear at nanotubes with diameters of greater than 1.1 nm. This inconsistent result may originate from the inhomogeneous distribution of nanotubes with different diameters in the bundle. Similar phenomena were also observed in ODA-treated samples.[5]

So far, we learned that the selective disintegration of m-SWCNTs is diameter dependent. In small-diameter nanotubes of less than 1.1 nm, both the strain effect and the abundance of charge density at the Fermi level play a dominant role for selective removal of metallic nanotubes. However, at large-diameter nanotubes of greater than 1.1 nm, the strain effect may be excluded. This strongly suggests that the selective adsorption on metallic nanotubes can be achieved by the abundant presence of charge density at the Fermi level and the extra strain effect should be accommodated in order to destroy the nanotube walls.

Terahertz (THz) conductivity measurements of SWCNT films on quartz substrates were performed to further prove the selective separation of s-SWCNTs. The dynamic response of the electrical conductivity for SWCNT films was measured using terahertz–time-domain spectroscopy (THz-TDS) in the frequency range of 0.2–2.0 THz. The THz-TDS is

based on the optoelectronic generation and detection of a beam of subpicosecond THz pulses.[28,29] The real conductivity as a function of THz was calculated from the measured index of refraction and power absorption as a function of THz.[30] Figure 7a shows the real conductivities of the pristine and the residual SWCNTs treated at 40 mmol of NHFA for 24 h as a function of THz frequency. The conductivities of both samples decreased with increasing frequency at the high-frequency region, following a simple Drude model, except not in the low-frequency region. This behavior has been explained by the influence of phonon absorption along the tube axis of s-SWCNTs.[28,29] What is more intriguing is that the real conductivity of the residual SWCNTs was reduced by about 30% consistently over all frequency ranges as compared to that of the pristine SWCNTs. Interestingly, the relative percentage of the conductivity reduction was close to that of the weight reduction observed during NHFA treatment. This reflects again the selective removal of m-SWCNTs, in agreement with Raman data.

The absorption spectra in the infrared and visible ranges can provide information for the metallicity of the entire sample, which cannot be obtained practically from finitely chosen excitation energies of the resonant Raman spectra. It is well established that the optical response of SWCNTs is dominated by transitions between peaks in the electronic density of states, with momentum conservation only allowing transition pairs of van Hove singularities with a mirror symmetry to the Fermi level.[31–33] Furthermore, the widths and fine structures of these absorption bands are specifically related to the distribution of diameters and chiralities of nanotubes.[34,35] The optical absorption spectra of the pristine SWCNTs and the residual SWCNTs treated at 40 mmol of NHFA for 24 h were compared in Fig. 7b to distinguish the metallicity between two samples. In the pristine SWCNTs, transitions between the first and second van Hove singularities (S_{11} and S_{22}) in s-SWCNTs were observed near 0.9 eV (S_{11}) and 1.5 eV (S_{22}), whereas the related peak (M_{11}) in m-SWCNT was observed near 2.0 eV. Although the nanodispersion of the pristine SWCNTs was insufficient in isopropyl alcohol followed by a drop casting on quartz substrate, several sub-band peaks in each band were clearly visible. On the other hand, several sub-band peaks in the NHFA-treated SWCNTs were suppressed due to the formation of large bundles during NHFA treatment, as shown in Fig. 2c and d. We note that the intensity of the M_{11} transition peak of the residual SWCNTs treated at 40 mmol of NHFA for 24 h was greatly suppressed due to the selective removal of m-SWCNTs. Moreover, the transition energies of the semiconducting peaks were all downshifted, suggesting that even for semiconducting nanotubes, some portions of the small diameter s-SWCNTs were also removed.

CONCLUSIONS

We have investigated a liquid-phase reaction using nitronium ions to remove metallic carbon nanotubes. We presented a separation technique that is capable of removing metallic nanotubes at small diameters of less than 1.1 nm with high yield. The s-SWCNTs remained intact with NHFA treatment, while the m-SWCNTs were completely destroyed and removed, especially for nanotubes with diameters close to or less than 1.1 nm. The nitronium ion selectively adsorbed on m-SWCNTs with higher binding energy by inducing a stronger charge transfer from nanotube to nitronium ion. This is due to the higher availability of electron density at the Fermi level of the metallic nanotubes, as compared to the counterpart s-SWCNTs. This difference becomes obscured for nanotubes with diameters greater than 1.1 nm. Our approach is straightforward without altering electronic structures during the treatment and is easily scalable to a large quantity process.

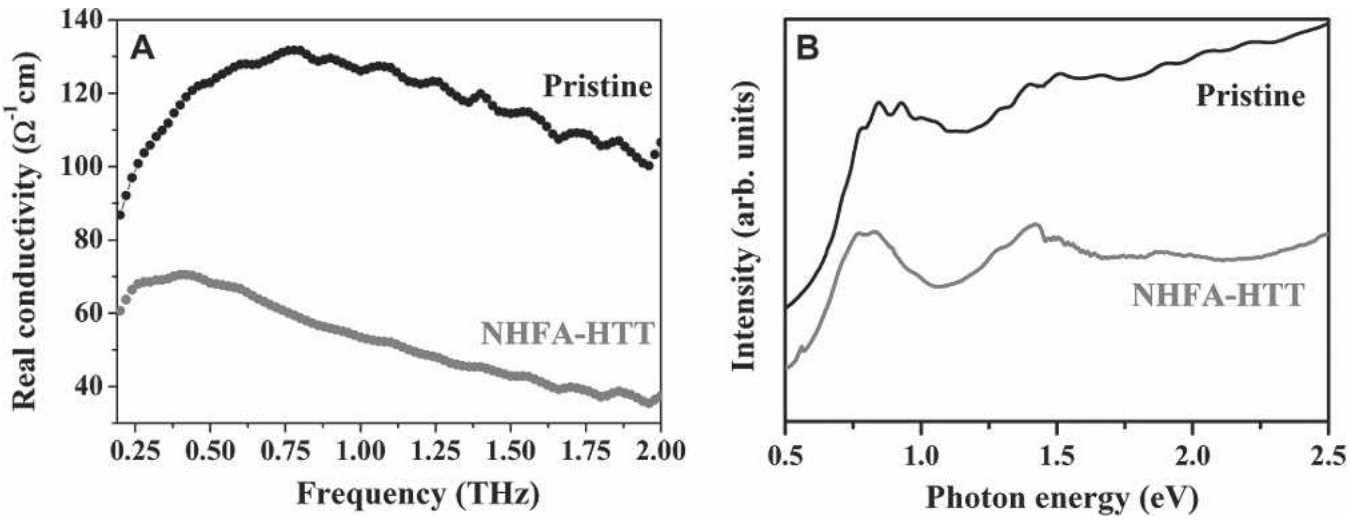

Fig. 7. (a) THz time-domain spectroscopy of the pristine sample and the NHFA treated residual SWCNTs with further heat treatment at 1,000°C (NHFA-HTT) in a vacuum and (b) the corresponding optical absorption spectra in the visible range.

ACKNOWLEDGEMENTS

This research was supported by Grant No. 05K1401-00412 from the Center for Nanoscale Mechatronics & Manufacturing, one of the 21st Century Frontier Research Programs, which are supported by the Ministry of Science and Technology in Korea, in part by the Center for Nanotubes and Nanostructured Composites at Sungkyunkwan University and in part by the Environmental Technology project of MOE.

REFERENCES

1. R. Krupke, F. Hennrich, H.V. Löhneysen, M. Manfred, and M.M. Kappes, *Science* 301, 344 (2003).
2. M. Zheng et al., *Science* 302, 1545 (2003).
3. D. Chattopadhyay, I. Galeska, and F. Papadimitrakopoulos, *J. Am. Chem. Soc.* 125, 3370 (2003).
4. Z. Chen, X. Du, C.D. Rancken, H.-P. Cheng, and A.G. Rinzler, *Nano Lett.* 3, 1245 (2003).
5. G.G. Samsonidze, S.G. Chou, A.P. Santas, V.W. Brar, G.F. Dresselhaus, M.S. Dresselhaus, A. Selbot, A.K.S. Ünlü, B.B. Goldberg, D. Chattopadhyay, S.N. Kim, and F. Padadimitrakopoulos, *Appl. Phys. Lett.* 85, 1006 (2004).
6. K.S. Kim, D.J. Bae, J.R. Kim, K.A. Park, S.C. Lim, J.-J. Kim, W.B. Choi, C.Y. Park, and Y.H. Lee, *Adv. Mater.* 14, 1818 (2002).
7. K.H. An, J.G. Heo, K.G. Jeon, D.J. Bae, C. Jo, C.W. Yang, C.-Y. Park, and Y.H. Lee, *Appl. Phys. Lett.* 80, 4235 (2002).
8. K.H. An, K.A. Park, J.G. Heo, Lim S.C. Jeon, C.W. Yang, Y.S. Lee, and Y.H. Lee, *J. Am. Chem. Soc.* 125, 3057 (2003).
9. M.S. Strano, C.A. Dyke, M.L. Usrey, P.W. Barone, M.J. Allen, H. Shan, C. Kittrell, R.H. Hauge, J.M. Tour, and R.E. Smalley, *Science* 301, 1519 (2003).
10. M. Yudasaka, M. Zhang, and S. Iijima, *Chem. Phys. Lett.* 374, 132 (2003).
11. S. Banerjee and S.S. Wong *Nano Lett.* 4, 1445 (2004).
12. W.C. Forsman and H.E. Mertwoy, *Synth. Met.* 2, 171 (1980).
13. K.H. An, K.A. Park, J.G. Heo, J.Y. Lee, Ku K. Jeon, S.C. Lim, C.W. Yang, Y.S. Lee, and Y.H. Lee, *J. Am. Chem. Soc.* 125, 3057 (2003).
14. H.C. Choi, S.Y. Kim, W.S. Jang, S.Y. Bae, J. Park, K.L. Kim, and K. Kim, *Chem. Phys. Lett.* 399, 255 (2004).
15. T.I.T. Okpalugo, P. Papakonstantinou, H. Murphy, J. McLaughlin, and N.M.D. Brown. *Carbon* 43, 153 (2004).
16. S. Biniak, G. Szymański, J. Siedlewski, and A. Światkowski, *Carbon* 35, 1799 (1997).
17. T. Hayashi, *Nano Lett.* 4, 1001 (2004).
18. D.W. Zeng, B.L. Zhu, C.S. Xie, W.L. Song, and A.H. Wang, *Mater. Sci. Eng. A* 366, 332 (2004).
19. H. Kuzmany, W. Plank, M. Hulman, C. Kramberger, A. Gruneis, T. Pichler, H. Perterlik, and Y. Achiba, *Eur. Phys. J. B* 22, 307 (2001).
20. H. Kataura, Y. Kumaza, Y. Maniwa, I. Umezu, S. Suzuki, Y. Ohtsuka, and Y. Achiba, *Synth. Met.* 103, 2555 (1999).
21. S.D.M. Brown, A. Jorio, P. Corio, M.S. Dresselhaus, G. Dresselhaus, R. Saito, and K. Kneipp, *Phys. Rev. B: Condens. Matter Mater. Phys.* 63, 155414 (2000).
22. L. An, Q. Fu, C. Lu, and J. Liu, *J. Am. Chem. Soc.* 126, 10520 (2004).
23. A. Kukovecz, T. Pichler, R. Pfeiffer, and H. Kuzmany, *Chem. Commun.* 1730 (2002).
24. A. Kukovecz, T. Pichler, C. Kramberger, and H. Kuzmany, *Chem. Commun.* 5, 582 (2003).
25. L. Kavan and L. Dunsxh, *Nano Lett.* 3, 969 (2003).
26. D.-H. Oh and Y.H. Lee, *Phys. Rev. B* 58, 7407 (1998).
27. K. Seo, C. Kim, K.A. Park, S. Han, B. Kim, and Y.H. Lee, submitted to *J. Am. Chem. Soc.* (2005).
28. T.-I. Jeon, K.-J. Kim, C. Kang, S.-J. Oh, J.-H. Son, K.H. An, D.J. Bae, and Y.H. Lee, *Appl. Phys. Lett.* 80, 3403 (2002).
29. T.-I. Jeon, K.-J. Kim, C. Kang, S.-J. Oh, J.-H. Son, K.H. An, J.Y. Lee, and Y.H. Lee, *J. Appl. Phys.* 95, 5736 (2004).
30. L. Duvilaret, F. Garet, and J.-L. Coutaz, *IEEE J. Selected Topics Quantum Electron.* 2, 739 (1996).
31. J.W. Mintmire and C.T. White, *Phys. Rev. Lett.* 81, 2506 (1998).
32. R. Saito, G. Dresselhaus, and M.S. Dresselhaus, *Phys. Rev. B* 61, 2981 (2000).
33. S. Reich and C. Thomsen, *Phys. Rev. B* 62, 4273 (2000).
34. M.E. Itkis, D.E. Perea, S. Niyogi, S.M. Rickard, M.A. Hamon, H. Hu, B. Zho, and R.C. Haddon, *Nano Lett.* 3, 309 (2003).
35. X. Liu, T. Pichler, M. Knupfer, M.S. Golden, J. Fink, H. Kataura, and Y. Achiba, *Phys. Rev. B* 66, 045411 (2002).